Transcription of Giant DNA Complexed with Cationic Nanoparticles as a Simple Model of Chromatin

Anatoly A. Zinchenko, François Luckel, and Kenichi Yoshikawa
Graduate School of Science, Department of Physics, Kyoto University, Sakyo-ku, Kyoto 608-8501, Japan; and "Spatio-Temporal Order" Project, International Collaboration Research Project, Japan Science and Technology Agency, Tokyo, Japan

ABSTRACT We prepared complexes of giant double-stranded DNA with cationic nanoparticles of 10–40 nm in diameter as an artificial model of chromatin and characterized the properties of changes in their higher-order conformation. We measured the changes in transcriptional activity that accompanied the DNA conformational transitions. Complete inhibition was found at excess concentrations of nanoparticles. In contrast, at intermediate stages of DNA binding with nanoparticles, the transcription activity of DNA survived, and this strongly depended on the size of the nanoparticles. For large nanoparticles of 40 nm, a decrease in transcriptional activity can be caused by the addition of only a small amount of nanoparticles. On the other hand, there was almost no inhibition of DNA transcriptional activity with the addition of small nanoparticles (10 nm) until very high concentrations, even under conditions that induced DNA compaction as revealed by single-DNA observation. At higher concentrations of 10-nm nanoparticles, DNA transcription activity decreased abruptly until it was completely inhibited. These results are discussed in relation to the actual size of the histone core, together with the mechanism of switching of transcriptional activity in eukaryotic cells.

INTRODUCTION

Recently, nanoparticles have attracted growing attention for their use in gene delivery and are currently considered to be prospective future vectors for biological and biomedical applications, including the transfection and transcription of genetic information (1–6). Studies on the fundamental characteristics of such systems are currently quite important and should provide valuable information for the further development of these applications. On the other hand, DNA-nanoparticle complexes are potential candidates for the biomimetic modeling of chromatin-like structures at different levels of organization, such as a ''beads-on-a-string'' structure and closed chromatin fibers.

Very recently, we reported a system which consists of a long T4 bacteriophage DNA chain associated with positively charged nanoparticles (7). Such DNA-nanoparticle complexes resemble natural DNA-histone complexes in many respects. In particular, ''DNA condensation'' with cationic nanoparticles is optimal at physiological salt conditions (0.1–0.5 M) and compaction of DNA can be realized by the wrapping of chains around nanoparticles. The biological relevance and functional biomimetism of this system is of great significance. As a next step, it is important to investigate the biological activity of long DNA incorporated into complexes with cationic nanoparticles, and in this study we examined the transcriptional activity of DNA upon binding with cationic nanoparticles. We showed how the compaction of giant bacteriophage DNAs (48 and 166 kbp) by nanoparticles of 10–40-nm sizes influences the transcriptional activity of DNA at the level of the molecular ensemble of DNA, as well as at the level of single DNA molecules. We have found that the transcriptional activity of DNA in DNA-nanoparticle complexes depends on the concentration and size of these particles, which suggests that different mechanisms for the inhibition of DNA transcription can be realized depending on the size of the interacting nanoparticles.

METHODS AND MATERIALS

Nanoparticles were prepared by the adsorption of poly(L-lysine) (molecular weight 30,000–70,000) that had been previously labeled by the modification of amino groups by the fluorescent dye Rhodamine Red X (Molecular Probes, Eugene, OR; adsorption and emission maxima 570/590 nm) on silica nanoparticles (Nissan Chemicals, Tokyo, Japan, Organoxasol series). We used three sets of nanoparticles with different sizes: S (10 nm), M (15 nm), and L (40 nm). The nanoparticles are similar to those used in our previous study (7).

Measurement of transcriptional activity

The transcriptional activity of bacteriophage T4 DNA (T4GT7 DNA, Wako, Nippon Gene, 166 kbp) was evaluated using an experimental protocol similar to that described previously (8). Transcription was performed in a solution containing 10 mM Tris-HCl buffer, 100 mM KCl, 5 mM $MgCl_2$, 0.1 mM adenosine triphosphate (ATP), cytidine triphosphate (CTP), and guanosine triphosphate (GTP), 0.01 mM γ-AmNS uridine triphosphate (UTP) (Molecular Probes, absorption/emission maxima ~330/463 nm), and 2 mM dithiothreitol. The DNA concentration was adjusted to be as low as possible (0.03 ng/100 μl). A variable concentration of nanoparticles was added, and samples were gently mixed before the addition of 1 U *Escherichia coli* RNA polymerase. These mixtures were then incubated at 37°C for 2 h. During RNA polymerization, the AmNS group is released in the bulk and becomes fluorescent. The final intensity of fluorescence is proportional to the amount of RNA polymerized and was measured in arbitrary units at 475 nm using a spectrofluorimeter.

Submitted July 31, 2006, and accepted for publication November 7, 2006.

Address reprint requests to Anatoly A. Zinchenko, E-mail: zinchenko@urban.env.nagoya-u.ac.jp.

0006-3495/07/02/1318/08 $2.00

doi: 10.1529/biophysj.106.094185

Compaction curves

Compaction curves were recorded in the same solutions as used for the measurement of transcriptional activity with the addition of the fluorescent dye DAPI (4′,6-diamidino-2-phenylindole; 0.1 μM) for DNA visualization.

Single-molecule observations

Reaction solutions of 40 μL containing 0.5 mM of ATP, CTP, GTP, 0.4 mM uridine 5′-triphosphate (UTP), 1 μM Chromatide Alexa Fluor 488-5-UTP (Molecular Probes; adsorption/emission maxima 495/519 nm), T7 transcription buffer provided with the polymerase kit, 1 μL DAPI (10 μM, Abs/Em 350/420 nm), and 10 ng λ ZAP II DNA (40 kbp, Stratagene) were prepared and mixed before the addition of variable concentrations of nanoparticles, and 1 U of T7 RNA polymerase (Invitrogen, Carlsbad, CA). Samples were incubated at 37°C for 2.5 h. Before microscopic observations, samples were stained again with 1 μL DAPI (10 μM) and observed by a Zeiss Axiovert (Jena, Germany) 135 television (TV) microscope equipped with a 100× oil-immersed lens and recorded on S-VHS (super-video home system) videotapes through a Hamamatsu (Hamamatsu, Japan) silicon intensifier target TV camera. For the observation of T4 DNA and nanoparticles, three different filters (Zeiss, Filter sets Nos. 2, 10, and 15) were used.

RESULTS AND DISCUSSION

Compaction of T4 DNA by cationic nanoparticles of different sizes

First, we observed the conformational behavior of fluorescence-labeled giant T4 DNA in solutions with different amounts of nanoparticles by fluorescent microscopy. Cationic nanoparticles with average sizes of 10 nm (S), 15 nm (M), and 40 nm (L) were examined with regard to the efficiency of DNA compaction. Fig. 1 shows the change in the conformation state of giant T4 DNA with the addition of cationic nanoparticles of 40 nm (L) to DNA solution. In the absence of nanoparticles, DNA moves freely in solution and shows translational Brownian motion, as shown in Fig. 1 *A*. With the addition of nanoparticles, DNA coils gradually decrease in size (Fig. 1, *B* and *C*) and intrachain fluctuations finally disappear, indicating that DNA adopts a compact state (Fig. 1, *D* and *E*). At L-nanoparticle concentrations higher than 1×10^{-3} wt %, all of the individual DNA chains in solution became associated with nanoparticles to form condensates. A similar decrease in the effective molecular volume of DNA and successive compaction was observed when smaller M and S nanoparticles were added to DNA. Fig. 2 *A* shows DNA compaction curves with L, M, and S nanoparticles based on the results of fluorescent microscopy observations. Each compaction curve shows the change in the conformation of DNA with the addition of nanoparticles in terms of the percentage of completely compacted DNA chains (as shown in Fig. 1, *D* or *E*) in the analyzed ensemble of DNA chains. Although such DNA compaction curves show the population of final compact DNA complexes, the interaction between DNA and nanoparticles starts earlier and is observed as a decrease in DNA coil size. Electrostatic interaction between the negatively charged phosphate groups of DNA and the positively charged amino groups of nanoparticle surfaces leads to the formation of polymer-colloid complexes between DNA and nanoparticles. Although all of the nanoparticles induce a transition in the DNA conformation into a compact form (Fig. 2 *A*), the concentration regimes of these transitions depend on the size of the nanoparticles. In good agreement with previous observations (7), the compaction potential of large (L) nanoparticles is the highest, after the weight concentration of nanoparticles is normalized by the available nanoparticle cationic surface area. Thus, L particles are more effective in terms of the charge ratio between DNA and nanoparticle ionogenic groups, since at the same weight concentrations, L particles have a smaller surface than M particles with a similar surface density. The smallest S nanoparticles are the least effective for DNA compaction. The effect of nanoparticle size on the efficiency of DNA compaction has been discussed in another article

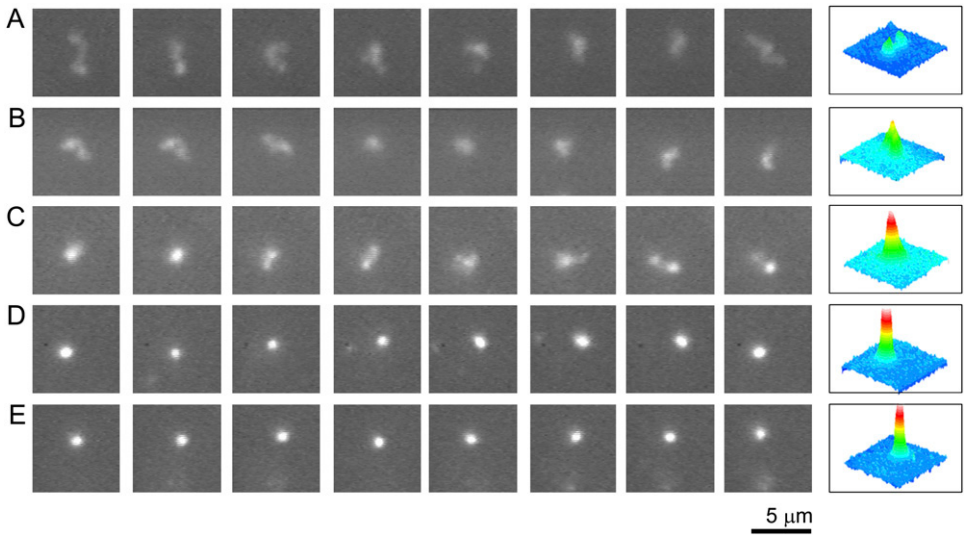

FIGURE 1 Fluorescence microscopic observation of the Brownian motion of single T4 DNA molecules at different concentrations of L nanoparticles observed in a solution of transcription buffer and the fluorescent dye DAPI. The nanoparticle concentration is 0 M (*A*), 1×10^{-4} wt % (*B*), 2.5×10^{-4} wt % (*C*), 5×10^{-4} wt % (*D*), and 1×10^{-3} wt % (*E*). The interval between frames is 0.4 s. The last column shows quasi-three-dimensional (3D) profiles of fluorescence for DNA at different degrees of DNA compaction by L nanoparticles derived from the first fluorescent images in the time sequences on the right.

(7). Briefly, the lower DNA compaction efficiency of smaller nanoparticles is attributed to different mechanisms of DNA chain complexation with nanospheres: the adsorption of DNA on L nanoparticles, the wrapping of DNA around M nanoparticles, and the decorating of DNA chains by S nanoparticles as a result of correlation between the DNA persistence length and nanoparticle sizes.

Changes in DNA transcriptional activity in complexes with cationic nanoparticles

The results of fluorescence spectroscopy measurements of the transcriptional activity of T4 DNA in complexes with L, M, and S nanoparticles of different concentrations under the same experimental conditions as used for fluorescent microscopy (FM) observations are shown in Fig. 2 *B*. The transcriptional activity of T4 DNA was evaluated by a fluorescent method described previously, which is based on measurements of changes in aminonaphthalenesulfonate fluorescence, attached to the terminal group of UTP, upon its release into bulk solution during RNA polymerization. Regardless of the size of the nanoparticles, the transcriptional activity of T4 DNA decreases with the addition of nanoparticles, and at a certain concentration of nanoparticles transcription is completely inhibited. Fig. 2 *B* shows that all of the transcription curves have three distinct regions. In the first region, transcriptional activity is almost preserved or only very slightly decreased. In the second region, a decrease of transcriptional activity is observed, and in the third region transcription is completely inhibited (zero fluorescence intensity). When we compare Fig. 2 *A* and Fig. 2 *B*, there is a direct correlation between the concentration regimes in DNA compaction by L, M, and S nanoparticles and those in DNA transcription experiments. Concentrations of L and M particles to induce DNA compaction are very similar, and inhibition of DNA transcription by L and M nanoparticles also occur at very similar weight concentrations. In contrast, DNA compaction and transcription activity inhibition require ~10 times higher concentrations of S nanoparticles than L or M.

If we compare the concentrations at which DNA compaction and the inhibition of DNA transcriptional activity occur (Fig. 2, *A* and *B*), in the case of L and M particles these concentrations are quite close and the major decrease in DNA transcriptional activity is a result of DNA compaction into final condensates. It should be emphasized again that although DNA compaction curves show the formation of the final compact state of DNA (i.e., compact DNA complexes without an unfolded DNA chain), the complexation of DNA with nanoparticles begins at much lower concentrations of nanoparticles. Therefore, these results indicate that the inhibition of DNA transcriptional activity begins at concentrations at which a large number of nanoparticles interact with the DNA scaffold. Further important conclusions can be made by analyzing the shape of transcription curves and the concentrations at which DNA transcription activity is inhibited in relation to DNA compaction. It has been confirmed that final condensates of long T4 DNA and nanoparticles contain different numbers of nanoparticles as determined by the nanoparticle size and the flexibility of DNA chains under particular experimental conditions. When DNA is compacted with L nanoparticles, the final DNA-nanoparticle condensates contain several tens of L nanoparticles per T4 DNA chain; in the case of M nanoparticles, there are more than 100 M nanoparticles per DNA chain, and over 1000 S nanoparticles are associated with a single DNA in a final compact complex. Taking into account the large number of nanoparticles in final DNA complexes, it becomes clear that significant inhibition is achieved only when DNA molecules

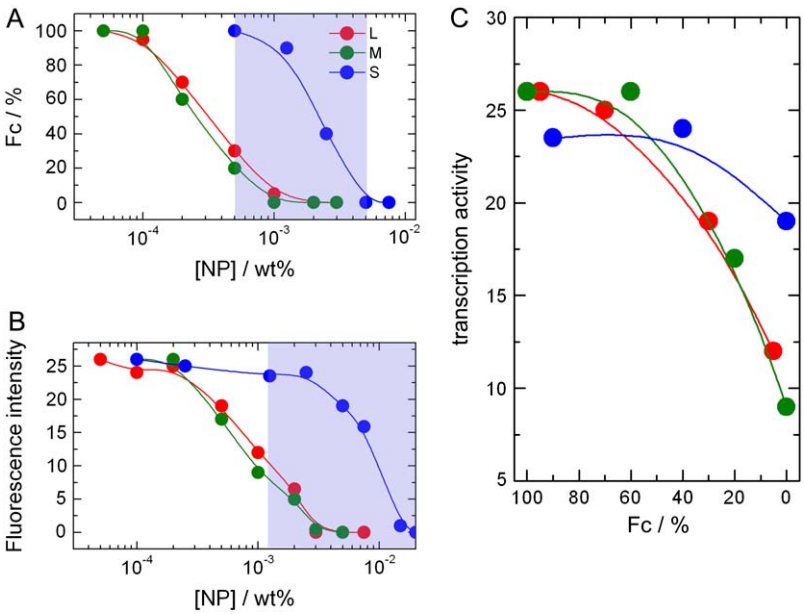

FIGURE 2 (*A*) Proportion of fully compact DNA F_c as a function of the nanoparticle concentration for L (*red*), M (*green*), and S (*blue*) nanoparticles. T4 DNA (1×10^{-6} M) labeled with the fluorescent dye DAPI (1×10^{-7} M) in the transcription buffer was used for observations. (*B*) Fluorescence intensity of aminonaphthalenesulfonate depending on the nanoparticle concentration: L (*red*), M (*green*), and S (*blue*) nanoparticles. The shaded region in *A* and *B* shows the S nanoparticles concentration ranges of changes in the conformation of DNA and changes in DNA transcriptional activity for comparison. (*C*) Dependence of transcriptional activity of T4 DNA in complexes with cationic nanoparticles on the degree of DNA compaction.

are loaded to a high extent with nanoparticles (Different DNA molecules in ensemble are evenly loaded with nanoparticles according to our transmission electron microscopy (TEM) observations). Fig. 2 *B* shows that if the nanoparticles are large (L), even small amounts of nanoparticles inhibit the transcriptional potential of DNA. The steeper slope of the transcription activity curve for S nanoparticles indicates that the inhibition of DNA transcriptional activity is an abrupt process and occurs only at the final stages of DNA complexation with nanoparticles.

The presence of a plateau in the transcription curves indicates that there is a threshold of DNA loading by nanoparticles for the initiation of a notable decrease in transcription activity. In the same way as described above, the inhibition of DNA transcriptional activity by L particles begins with the addition of the first L nanoparticles, i.e., at concentrations ~30 times smaller than the final nanoparticle concentration necessary for complete DNA compaction. In contrast, the plateau in the transcription curve for S nanoparticles is very long and shows a very steep final inhibition. There is an ~5-fold difference between the concentrations at which S can initiate notable inhibition and completely inhibit DNA transcription. The case with M nanoparticles lies between those with L and S.

It is useful to represent DNA transcriptional activity as a function of the degree of DNA compaction, as shown in Fig. 2 *C*. These curves show that the formation of DNA compact complexes with L or M particles almost completely inhibits transcription activity, whereas the compaction of DNA with S nanoparticles inhibits DNA transcriptional activity only partly, and complete inhibition takes place at higher concentrations of nanoparticles. Also note that the inhibition of DNA transcription by L nanoparticles starts earlier than with M nanoparticles.

Based on the parallel FM and fluorescent spectroscopy observations, an important conclusion is the ability of long DNA to remain biologically active even when it is complexed with a large number of cationic nanospheres, and thus compacted. This preservation of DNA transcription activity is especially remarkable for S nanoparticles.

Single-molecule observation of DNA transcription in complexes with nanoparticles

In this study, we also sought to independently determine the correspondence between the degree of DNA compaction and DNA transcriptional activity at the level of single DNA molecules. We performed another set of fluorescent microscopy observations to find the correlation between the conformational state of DNA, the degree of DNA complexation with nanoparticles, and the amount of transcribed RNA. For these experiments, we used another giant DNA, λ ZAPII, which has a specific T7 promoter at approximately the center of the DNA chain. To monitor RNA production, Alexa Fluor-labeled UTP was added to the conventional transcription buffer. Upon transcription, Alexa-UTP is polymerized into final RNA, which makes possible fluorescent observation of the transcription product at high degrees of polymerization. Therefore, three components of our system—DNA, nanoparticles, and transcribed RNA, each labeled with distinct fluorescent dyes—can be monitored simultaneously by using three different fluorescent filters (see Methods and Materials), which will be referred to as the DNA filter, RNA filter, and nanoparticle filter, respectively.

The change in the long-axis length of λ-DNA at different concentrations of added S nanoparticles is illustrated in Fig. 3. As with changes in the conformation of T4 DNA, the addition of S nanoparticles to a solution of λ-DNA leads to gradual shrinking of the DNA image and the continuous compaction of DNA coils into globules (Fig. 4 *E*) at an S concentration of 0.01 wt %, after which no further changes in the size of DNA are detected. A similar change in DNA conformation can be observed with M and L nanoparticles.

In bulk experiments, no information about RNA transcription can be obtained due to the small size and comparatively low fluorescence signal from the RNA chain involved

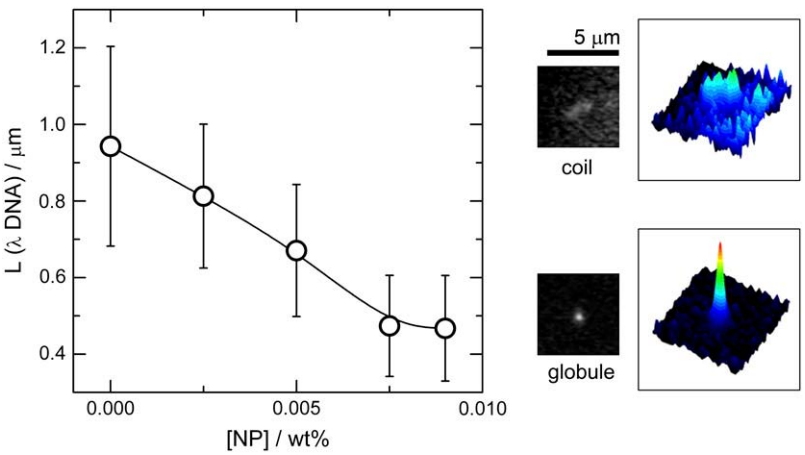

FIGURE 3 Change in the average long-axis length of λ-DNA as a function of the concentration of S nanoparticles, deduced from single-DNA observation by fluorescence microscopy. At least 100 DNA molecules were analyzed for each concentration of nanoparticles. Images on the right are quasi-3D profiles of fluorescence for DNA at different degrees of DNA compaction by L nanoparticles derived from the first fluorescent images in time sequences on the right.

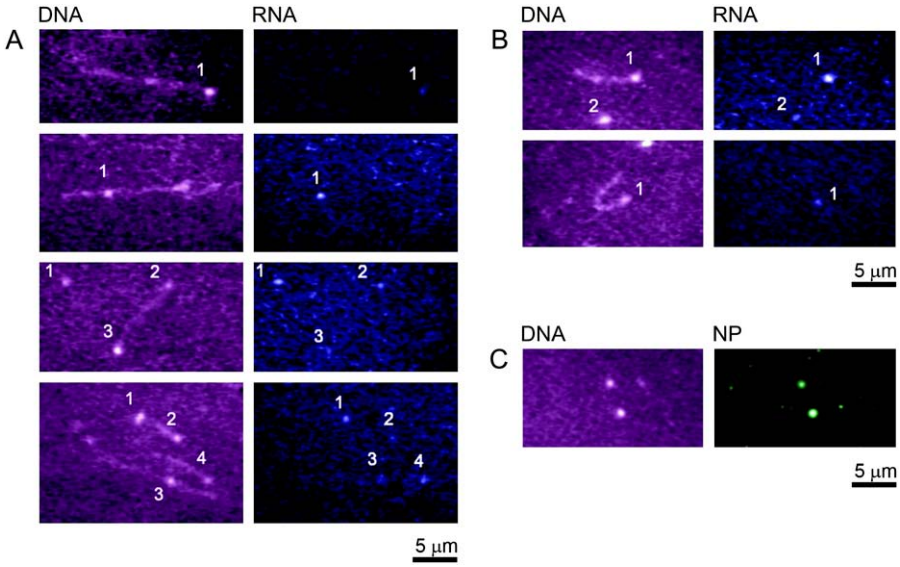

FIGURE 4 Fluorescent images (false color) of λ-DNA in the absence (*A*) and presence of different amounts of S nanoparticles ((*B*) 2.5×10^{-3} wt % and (*C*) 7.5×10^{-3} wt %) as observed through different fluorescent filters to visualize DNA and RNA transcripts separately. Pairs of images correspond to the same observation area. The names of columns, ''DNA'', ''RNA'', and ''NP'', indicate the type of fluorescent filter used and do not necessarily refer to the object observed in the actual experiment.

in Brownian motion. Fluorescence from nanoparticles is observed at later stages of DNA chain compaction (0.005 wt % of S in the observations described above), which highlights the fluorescent profile from DNA chains labeled with DAPI. A stretching operation to deposit RNA molecules on glass is essential for the successful observation of both DNA and RNA fluorescent images. We performed stretching on a droplet of sample solution used for bulk experiments (Figs. 4 and 5). In a solution without nanoparticles we observed stretched λ-DNA molecules as shown in Fig. 4 *A* through the DNA filter. On most DNA molecules, bright spots were found, which are indicated by numbers. The location of these dots on DNA chains is arbitrary. Bright spots as shown in Fig. 4 *A* (the third pair of images) were also observed coexisting with stretched λ-DNA molecules. The number of such free dots is dependent on the time of transcription. Fig. 4 *A* (*left column*, *blue color images*) shows the corresponding fluorescent images observed with the RNA filter, and it is possible to make a correspondence between the location of bright spots on the DNA and RNA molecules. We found that all of the fluorescent dots of RNA correspond to the dots on DNA and in a free state as observed through the DNA filter. This may be the result of DAPI labeling of RNA molecules. Finally, we made a control observation through the nanoparticle filter to confirm that no fluorescent objects were observed in nanoparticle-free solution.

Further experiments were performed with the addition of S nanoparticles to λ-DNA without changes in other experimental parameters. Fig. 4 *B* illustrates single-molecule fluorescent observations performed at 2.5×10^{-3} wt % of S nanoparticles, which corresponds to the partially shrunken DNA coils in bulk experiments. At this concentration, fluorescent images observed through the DNA filter were similar to those in a free DNA sample: unfolded DNA chains with dots as well as free dots (Fig. 4 *B*). However, an important difference was the shorter length of stretched DNA, probably as a result of complexation with S nanoparticles. Through the RNA filter we observed RNA dots, which, as described above, highlighted dots observed through the DNA filter. Slightly fewer RNA dots were observed compared to the number of RNA fluorescent dots observed in the experiment with uncomplexed DNA. At this concentration of S nanoparticles, fluorescent images were still not observed through the nanoparticle filter due to low fluorescence from individual small nanoparticles and comparatively low loading of the DNA chain with the nanoparticles. A further increase in the nanoparticle concentration induces DNA shrinking and a decrease in the number of observed RNA fluorescent dots.

Finally, at an S concentration of 7.5×10^{-3} wt %, DNA was completely compacted and through the DNA filter we observed only globules, as shown in Fig. 4 *C*. Fig. 4 *C* also shows corresponding fluorescent images observed using the nanoparticle filter and corresponds to the fluorescent profile

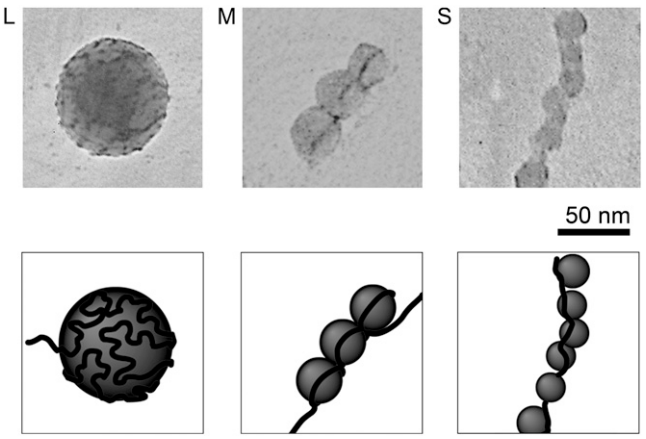

FIGURE 5 Electron microscopic observation, TEM, of T4 DNA complexes with L, M, and S nanoparticles and schematic representations of the complexes.

from nanoparticles. All of the observed DNA globules have a corresponding signal from nanoparticles, indicating that DNA has been compacted due to complexation with nanoparticles. When DNA is compact, no corresponding RNA dot signal was found using the RNA filter. However, our spectroscopic measurements indicate significant RNA production even when DNA is compacted at this concentration. Although we did not observe RNA as fluorescent dots under conditions in which DNA was compacted, it is possible that transcription is not inhibited, but the products of such transcription, which can be shorter RNA molecules, may be difficult to monitor under the present conditions due to signal limitations.

DISCUSSION

Our past studies on the correlation between the conformational state of DNA and biological activity in DNA compaction by multivalent cations showed that the compaction of long DNA into an ordered and dense state by the polyamine spermine (3+) results in the complete inhibition of DNA transcription activity (9,10). Such inhibition proceeds in an all-or-none manner, which reflects the fact that DNA compaction with multications is a first-order phase transition. Whereas DNA compaction by multications leads to extremely tight packaging, similar to DNA packaging in bacteriophages (11), a completely different scenario is realized in eukaryotic cells, including human cells, where histone octamers and other cationic scaffolds provide hierarchic compaction of DNA chains into chromatin (12). The cationic nanoparticles used for our study are primitive analogs of histone core particles and, thus, the whole system which includes long DNA and nanoparticles allows us to gain deeper insight into the biological functionality of DNA during chromatin-like compaction in a model system. There have been several reports on DNA complexation with cationic nanoparticles with regard to DNA transcriptional activity, and it has been demonstrated that DNA transcriptional activity is inhibited upon complexation with nanoparticles (13), but no systematic study has been performed.

Based on experiments on natural systems, it is well known that there is a correlation between the transcriptional activity of DNA in complexes with histones and the degree of acetylation of histones (14). For example, binding of DNA with nonacetylated histones leads to the complete inhibition of DNA transcriptional activity (15–17). The first model of histone octamers was realized by cationic dendrimers—spherical macrocations that measure from a few to ~10 nanometers. An analysis of changes in the transcriptional activity of DNA upon DNA complexation with dendrimers revealed that DNA transcriptional activity is completely inhibited with the addition of dendrimers (18). The investigation of DNA binding with dendrimers of different sizes demonstrated that the complexes formed with either larger or smaller dendrimers at the same charge ratios inhibited DNA transcriptional activity equally. In contrast, in our study we found that such inhibition depends on the nanoparticle size and that larger nanoparticles more significantly inhibit DNA compaction activity.

The difference between nanoparticles with regard to their ability to inhibit transcription is related to the mechanism of nanoparticle interaction with DNA. Since the long chain of double-stranded DNA is a semiflexible polyelectrolyte, the correlation between the persistence length of DNA and the size of nanoparticles leads to different scenarios of DNA chain arrangement on the surface of a nanoparticle. Two different models of DNA complexation can be suggested for L, M, and S nanoparticles. Since L nanoparticles are large enough, DNA chains adsorb freely and, due to a large number of salt bonds, irreversibly, on the surface of nanoparticles. In contrast, the size of S nanoparticles does not allow DNA chains to adsorb or even wrap around a 10-nm nanosphere, and thus the only possible manner of complexation is the adsorption of nanoparticles on a DNA chain.

Transmission electron micrographs of complex fragments, where DNA is complexed with L, M, and S nanoparticles, are shown in Fig. 5 together with schematic illustrations of complex models. If nanoparticles are large, e.g., L nanoparticles (Fig. 5 *L*), a large amount of the DNA chain is adsorbed on the surface of cationic nanoparticles and such complexation suggests strong and almost irreversible adsorption of a DNA chain on the nanoparticle surface. Such interaction is expected, in turn, to inhibit polymerase activity if a promoter site is located on an adsorbed part of a DNA chain or, when a promoter site is still available, to impede the slipping of polymerase along a DNA chain. Due to the intrinsic rigidity of DNA, a decrease in the nanoparticle size down to 15 nm (M) prevents the free adsorption of double-stranded DNA on M nanoparticles and DNA can only wrap around such nanoparticles, as shown in Fig. 5 *M*. Furthermore, the interaction of DNA with the smallest nanoparticles (S) can proceed only by the collection of nanoparticles on a DNA chain as shown in Fig. 5 *S*. This interaction suggests that the binding of DNA to S nanoparticles is reversible because no wrapping occurs and there are only a few binding sites. In this scenario, S nanoparticles can slip along DNA or dissociate, which makes the whole DNA chain accessible for polymerase functioning. The inhibition of transcription by S nanoparticles occurs at a final stage, when many S particles in a complex with DNA form a strong compact complex with large networks of bonds. In a recent report (19), it was suggested that if polymerase anchors to DNA, it can displace nanoparticles from the DNA surface during transcription. Since the nanoparticles used in this study were small, below 10 nm, we believe that such a mechanism is also realized at earlier stages of DNA interaction with S nanoparticles. M nanoparticles interact with DNA by wrapping the DNA double helix and in this scenario, which is very similar to the natural DNA-histone system, DNA is expected to be accessible to polymerase at intermediate stages of compaction (similar to a ''beads-on-a-string'' structure). According

to the results with a natural DNA-histone complex, 1.75-fold wrapping of a DNA chain around 7-nm histone proteins is reversible and well-known processes such as histone sliding (20) or unwrapping of either of the two DNA turns (21) are important mechanisms that provide access to DNA for reading genetic information. In this study, we found that M and, to a greater extent, S nanoparticles are different from L nanoparticles with regard to the length of the plateau in the transcription curve, where no inhibition occurs. This indicates that the DNA chain is more accessible in complexes with S and M nanoparticles than with L nanoparticles.

The scenarios that have been suggested for the movement of DNA polymerase along DNA for different nanoparticles are shown in Fig. 6. The complexation of DNA with large nanoparticles such as L inhibits the movement of polymerase because such complexation is very strong. M nanoparticles, which are wrapped by DNA, can slip along a DNA chain as in natural systems and thus provide a mechanism for the movement of polymerase. However, at higher degrees of DNA loading with particles, this motion may be inhibited, as in the case of L particles. This difference between L and M nanoparticles is supported by higher degrees of DNA compaction with M particles when transcription becomes inhibited than with L particles. On the other hand, the low binding constants for S nanoparticles with DNA allow polymerase motion and functioning until very high degrees of DNA complexation with nanoparticles, after which abrupt inhibition occurs. In addition, it should be mentioned that this model should also consider steric hindrance of polymerase positioning on DNA by bound nanoparticles as well as the appearance of certain steric obstacles for transcription processes when the molecular density of the DNA coil significantly decreases upon loading with nanoparticles.

Our model allows for simple numerical comparison of a mechanical work made by polymerase during motion along DNA by the distance equivalent to one nucleotide (elementary length of polymerase motion) and electrostatic contribution of the free energy of DNA interaction with nanoparticles having different sizes. With the help of single molecule force measurements it was found that ~2.5 kT energy is used for polymerase motion by one nucleotide; however the energy from a nucleoside triphosphate (NTP) hydrolysis reaction, which moves polymerase, is much higher, 12 kT, and thus

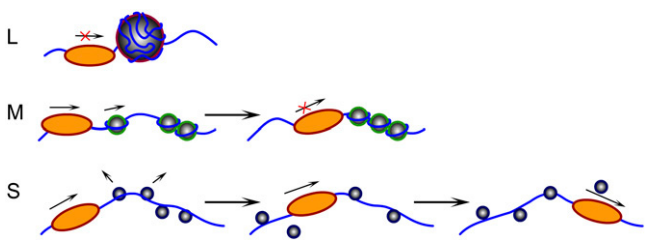

FIGURE 6 Schematic representations of three scenarios for the movement of DNA polymerase (*orange oval*) along a DNA chain complexed with nanoparticles of different sizes.

the efficacy of polymerase is ~20%. (22) On the other hand, electrostatic contribution to the free energy for each bond of DNA with an interacting polycation was estimated as 2 kT (23) (this value is probably overestimated). The number of cationic bonds can be estimated according to the charge density on NP (~1 e/nm^2), size of nanoparticles (NP), and mode of interaction. According to our model (Fig. 6), there are two possibilities for how particle can be displaced from the certain binding site on DNA by polymerase: dissociation of the nanoparticle from DNA or slipping of the NP along DNA. Due to nonwrapping mechanisms of interaction and small size, S nanoparticles interact with DNA forming only a few bonds, therefore, both slipping of particle along DNA and complete dissociation from DNA are possible when polymerase moves from the balance of polymerase work and electrostatic energy of DNA-NP interaction. Dissociation of M nanoparticles from DNA is certainly impossible because the number of bonds formed by DNA with M nanoparticle (calculated for one full DNA turn around the nanoparticle and a 15-nm average size) is ~50, and the corresponding electrostatic interaction is very high. However, the slipping of particle by simple repetitive dissociation of an ionic bond at the nearest location to the moving polymerase and formation of a new bond at the other end of the outgoing chain of DNA requires only 2 kT to maintain such a slipping. A similar slipping phenomenon takes place in vivo (24), and it was also confirmed by computer simulations (25). However, in the case of a sequence of DNA-wrapped particles on the DNA chain, this slipping activation energy should be multiplied by the number of particles in the sequence, suggesting that the sequence of several M particles should finally prevent polymerase from the motion. In the case of L nanoparticles, where the above-mentioned slipping is not possible due to the formation of a large number of salt bonds between DNA and the nanoparticle, neither of the mechanisms can be realized.

It is interesting to compare the changes in the transcriptional activity of DNA upon complexation with nanoparticles and the recently reported changes in DNA transcriptional activity upon condensation by low-molecular-weight multivalent cations such as spermine (8). When DNA interacts with spermine, as a result of the first-order phase transition of a long DNA chain from an elongated into a compact state, DNA undergoes on/off switching of transcriptional activity. Another important feature of this change in transcriptional activity is the increase in transcription at the earlier stages of DNA compaction by spermine and the abrupt disappearance of DNA transcription activity when DNA is compacted into globules. In contrast, when DNA is compacted with nanoparticles, we observed progressive loading of DNA chains with cationic nanoparticles, and this system did not show either an increase in the rate of transcription at earlier stages or a rapid disappearance of transcription. In contrast, when nanoparticles were added to the DNA chain, DNA transcription activity gradually decreased. Since in DNA compaction by

multications the compaction of DNA is accompanied by the total inhibition of DNA transcriptional activity, this difference is of particular interest for applications that require the compaction of DNA chains while preserving their biological functions.

The change in the transcriptional activity of DNA upon interaction with dendrimers (18) resembles the change in DNA transcription upon binding with multivalent cations such as spermine (8,9), i.e., it first increases and then decreases until it is completely inhibited. In contrast, DNA interaction with cationic nanoparticles and the manner of transcriptional activity inhibition observed in this study resemble the change in DNA transcriptional activity when DNA interacts with histones, where no initial increase is observed.

CONCLUSION

Changes in the transcriptional activity of giant DNA chains with the addition of cationic nanoparticles that measure 10–40 nm indicated that the transcriptional activity of DNA can be significantly preserved even when DNA chains are compacted as a result of interaction with cationic nanospheres. At high concentrations of nanoparticles, DNA transcriptional activity is completely inhibited. Larger nanoparticles showed more effective inhibition than smaller nanoparticles at lower DNA loading ratios. The ability of DNA-nanoparticle complexes, especially with small nanoparticles, to retain significant biological (transcriptional) activity upon compaction by cationic nanoparticles, as primitive models of histones, is an important step toward creating biomimetic structures of open chromatin. Our findings are expected to contribute to the modeling and preparation of new DNA vectors to construct complexes where DNA preserves significant biological activity even in a compact form.

Dr. D. Baigl (Ecole Normale Superieure) is acknowledged for help with nanoparticles preparation and electron microscope observations. Dr. T. Sakaue (Kyoto University) is acknowledged for fruitful discussions.

This work is partly supported by Grant-in-Aid for Scientific Research No. 18719001 from MEXT (Japan Ministry of Education, Culture, Sports, Science and Technology), Japan.

REFERENCES

1. Luo, D., and W. M. Saltzman. 2000. Synthetic DNA delivery systems. *Nat. Biotechnol.* 18:33–37.
2. Kneuer, C., M. Sameti, U. Bakowsky, T. Schiestel, H. Schirra, H. Schmidt, and C.-M. Lehr. 2000. A nonviral DNA delivery system based on surface modified silica-nanoparticles can efficiently transfect cells in vitro. *Bioconjug. Chem.* 11:926–932.
3. Luo, D., E. Han, N. Belcheva, and W. M. Saltzman. 2004. A self-assembled, modular DNA delivery system mediated by silica nanoparticles. *J. Controlled Release.* 95:333–341.
4. Thomas, M., and A. M. Klibanov. 2003. Conjugation to gold nanoparticles enhances polyethylenimines transfer of plasmid DNA into mammalian cells. *Proc. Natl. Acad. Sci. USA.* 100:9138–9143.
5. Li, Z., Z. Li, S. Zhu, K. Gan, Q. Zhang, Z. Zeng, Y. Zhou, H. Liu, W. Xiong, X. Li, and G. Li. 2005. Poly-L-lysine-modified modified silica nanoparticles: a potential oral gene delivery system. *J. Nanosci. Nanotechnol.* 5:1199–1203.
6. Roy, I., T. Y. Ohulchanskyy, D. J. Bharali, H. E. Pudavar, R. A. Mistretta, N. Kaur, and P. N. Prasad. 2005. Optical tracking of organically modified silica nanoparticles as DNA carriers: a nonviral, nanomedicine approach for gene delivery. *Proc. Natl. Acad. Sci. USA.* 102:279–284.
7. Zinchenko, A. A., K. Yoshikawa, and D. Baigl. 2005. Compaction of single-chain DNA by histone-inspired nanoparticles. *Phys. Rev. Lett.* 95:228101/1–228101/4.
8. Luckel, F., K. Kubo, K. Tsumoto, and K. Yoshikawa. 2005. Enhancement and inhibition of DNA transcriptional activity by spermine: a marked difference between linear and circular templates. *FEBS Lett.* 579:5119–5122.
9. Tsumoto, K., F. Luckel, and K. Yoshikawa. 2003. Giant DNA molecules exhibit ON/OFF switching of transcriptional activity through conformational transition. *Biophys. Chem.* 106:23–29.
10. Yamada, A., K. Kubo, T. Nakai, K. Tsumoto, and K. Yoshikawa. 2005. All-or-none switching of transcriptional activity on single DNA molecules caused by a discrete conformational transition. *Appl. Phys. Lett.* 86:223901.
11. Cerritelli, M. E., N. Cheng, A. H. Rosenberg, C. E. McPherson, F. P. Booy, and A. C. Steven. 1997. Encapsidated conformation of bacteriophage conformation of bacteriophage T7 DNA. *Cell.* 91:271–280.
12. Wolffe, A. P. 1998. Chromatin: Structure and Function. Academic Press, New York.
13. McIntosh, C. M., E. A. Esposito III, A. K. Boal, J. M. Simard, C. T. Martin, and V. M. Rotello. 2001. Inhibition of DNA transcription using cationic mixed monolayer protected gold clusters. *J. Am. Chem. Soc.* 123:7626–7629.
14. Matthews, H. R. 1993. Polyamines, chromatin structure and transcription. *Bioessays.* 15:561–566.
15. Chiou, H. C., M. V. Tangco, S. M. Levine, D. Robertson, K. Kormis, and C. H. Wu. 1994. Enhanced resistance to nuclease degradation of nucleic acids complexed to asialoglycoprotein-polylysine carriers. *Nucleic Acids Res.* 22:5439–5446.
16. Janne, O., C. W. Bardin, and S. T. Jacob. 1975. DNA-dependent RNA polymerases I and II from kidney. Effect of polyamines on the in vitro transcription of DNA and chromatin. *Biochemistry.* 14:3589–3597.
17. Frugier, M., C. Florentz, M. V. Hosseini, J.-M. Lehn, and R. Giege. 1994. Synthetic polyamines stimulate in vitro transcription by T7 RNA polymerase. *Nucleic Acids Res.* 22:2784–2790.
18. Bielinska, A. U., J. F. Kukowska-Latallo, and J. R. Baker Jr. 1997. The interaction of plasmid DNA with polyamidoamine dendrimers: mechanism of complex formation and analysis of alterations induced in nuclease sensitivity and transcriptional activity of the complexed DNA. *Biochim. Biophys. Acta.* 1353:180–190.
19. Han, G., N. S. Chari, A. Verma, R. Hong, C. T. Martin, and V. M. Rotello. 2005. Controlled recovery of the transcription of nanoparticle-bound DNA by intracellular concentrations of glutathione. Controlled recovery of the transcription of nanoparticle-bound DNA by intracellular concentrations of glutathione. *Bioconjug. Chem.* 16:1356–1359.
20. Gottesfeld, J. M., J. M. Belitsky, C. Melander, P. B. Dervan, and K. Luger. 2002. Blocking transcription through a nucleosome with synthetic DNA ligands. *J. Mol. Biol.* 321:249–263.
21. Kulic, I. M., and H. Schiessel. 2004. Chromatin dynamics: nucleosomes go mobile through twist defects. *Phys. Rev. Lett.* 92:228101.
22. Wang, M. D., M. J. Schnitzer, H. Yin, R. Landick, J. Gelles, and S. M. Block. 1998. Force and velocity measured for single molecules of RNA polymerase. *Science.* 282:902–907.
23. Korolev, N., A. P. Lyubartsev, and A. Laaksonen. 2004. Electrostatic background of chromatin fiber stretching. *J. Biomol. Struct. Dyn.* 22: 215–226.
24. Ura, K., J. J. Hayes, and A. P. Wolffe. 1995. A positive role for nucleosome mobility in the transcriptional activity of chromatin templates: restriction by linker histones. *EMBO J.* 14:3752–3765.
25. Sakaue, T., K. Yoshikawa, S. H. Yoshimura, and K. Takeyasu. 2001. Histone core slips along DNA and prefers positioning at the chain end. *Phys. Rev. Lett.* 87:078105.